Energies of strained vicinal surfaces and strained islands

V. M. Kaganer and K. H. Ploog
Paul-Drude-Institut für Festkörperelektronik, Hausvogteiplatz 5-7, D-10117 Berlin, Germany
(Received 27 March 2001; published 15 October 2001)

We show that the interaction between the strain field of a surface step with uniform strain gives rise to a negative line energy of steps. The energy of a vicinal surface under compressive strain is found to be lower than the energy of the singular-crystal facet. We consider the surface of a three-dimensional strained island as a stepped surface and derive the island's energy and equilibrium shape from step energies and step-step interactions under strain. We develop a kinetic model of the island growth as the motion of atomic steps forming the island surface. Mass transport to the island top is provided by attachment of adatoms to steps from the down terraces and detachment to the up terraces.

DOI: 10.1103/PhysRevB.64.205301 PACS number(s): 81.10.Aj, 68.35.Ct, 81.15.Hi

I. INTRODUCTION

The energetics of strained heteroepitaxial films has attracted enormous interest after it was found that the film can relax its elastic energy by forming small dislocation-free three-dimensional islands (Stranski-Krastanov growth).[1,2] The investigations are stimulated by potential applications of these islands as quantum dots in optoelectronic devices. The applications require dense arrays of uniform islands, which inspired numerous experimental and theoretical studies of the island growth and shape. Theoretical models[3–11] consider the competition between the released elastic energy and the extra surface energy. Approaches to evaluate the elastic energy are well established and involve either numerical finite-element calculations[8–11] or a very useful analytical approximation[3–5,12,13] applicable for small slopes of the island surface.

The surface energy is regarded either as being independent of the surface orientation[5,9,13] or the consideration is restricted to a limited number of predefined low-index facets with fixed orientations and surface energies.[3,4,10,11] The first approximation implies that the crystal is above the roughening temperature for the actual surface orientation. However, the Stranski-Krastanov growth is performed well below the roughening temperature. The applicability of the second approximation can be justified by the presence of the low-index dense-packed facets bounding the strained islands in systems with very large misfit, such as InAs/GaAs or InAs/InP.[14] However, systems with smaller misfits reveal high-index facets making smaller angles to the substrate surface. A notable example is the growth of Ge islands on Si(001). The islands obtained by molecular beam epitaxy develop (105) facets,[2] while the islands obtained by liquid phase epitaxy are (115) faceted.[15] Both orientations obviously do not correspond to a cusp in the orientational dependence of the surface energy of the unstrained Ge crystal. It is also worth to note that the treatment of low-index dense-packed facets together with the small-slope approximation for the elastic energy[3,4] implies that the low-index facets form small angles to the substrate surface. This means that it applies only to islands grown on high-index substrate surfaces.

In the present paper, we consider corrugated heteroepitaxial systems with moderate misfits, like $Si_xGe_{1-x}/Si(001)$, whose facets make small angles to the interface and can be treated as vicinal surfaces. We expect that such a treatment can be applied, at least qualitatively, even to the (105) or (115) facets of Ge/Si(001) islands mentioned above as being vicinal with respect to the (001) surface.

The energy of a vicinal surface is given by the line energies of the steps and the step-step interaction energies. A remarkable study of the step energies on strained surfaces was performed by Xie *et al*.[16] Their atomistic calculation of the steps on a strained Si(001) surface showed that the step energies are strongly influenced by the applied strain. The compressive strain gives rise to negative step energies, which explains the dependence of the roughening of strained films on the sign of the strain.[16,17] We show below that the results of Xie *et al*. can be understood in terms of linear elasticity, as an interaction of the strain field of the step with the uniform strain in the film. We express the energy of a strained vicinal surface by the step-step interaction energy on an unstrained surface. We find that, under compressive strain, the energy of a vicinal surface is lower than the energy of the singular surface.

The negative line energy of steps under compressive strain gives rise to step creation as a way of reducing the surface energy. Such a roughening of an initially singular facet is limited by the short-range step-step repulsion which makes small distances between steps unfavorable. Hence, under lateral compression, an initially flat singular facet can reduce its surface energy by developing surface undulations with a finite strain-dependent slope. We calculate the energy released by these undulations and estimate the surface slope.

We analyze the energy of three-dimensional strained islands obtained by Stranski-Krastanov growth. We consider axially symmetric islands with the surface consisting of concentric circular steps. We perform an exact calculation of the interaction energy between these circular steps. Previous investigations of the dynamics of an unstrained crystalline cone[18,19] approximated the interactions between circular steps by those of straight steps. Such an approximation, however, is valid only when the difference between the step radii is small compared to the radii. This condition is satisfied for steps on unstrained surfaces since the step-step interaction is short range (the interaction energy decays as x^{-2}, where x is the distance between steps). However, the interaction be-

tween steps on strained surfaces is long range (the interaction energy is proportional to $\ln x$) and an exact calculation is necessary.

We treat arbitrary axially symmetric islands. In describing the line energies of the steps on the surface of strained islands and their interactions, we take into account that the strain acting on a step is not the same for all steps but depends on the position of the step in the cone, as a result of strain relaxation at the island apex and strain concentration at its bottom. The faceting of the island is modeled by the surface consisting of one or two straight segments in cross section. In the simplest case, our general formulas agree with those of Tersoff *et al.*[3] who considered pyramids, but substantially differ in specifying the surface energy.

We finally develop a kinetic model of island growth by extending the model which we have initially proposed for straight steps[20] to the case of circular steps. We follow the familiar Burton-Cabrera-Frank step kinetics equations[21–23] with the appropriate modification for circular steps.[18,19] The island growth proceeds by attachment of adatoms from the wetting layer. The material transport to the island top is provided by attachment of adatoms to the steps from down terraces and detachment to up terraces. New atomic layers are created on the island top if the step that bounds it is able to expand. We show that the negative line energy of the step on the compressed film mentioned above gives rise to the expansion of the top layer and hence to the growth of the island. This behavior is mediated by the strain and is not possible for unstrained islands which can only contract in time.[18,19] We find that the shapes and energies of the islands obtained with this kinetic model differ from those of islands obtained by energy minimization. The size of a nucleus necessary for island growth significantly differs from the one reducing the energy. Hence, energy minimization is not sufficient to describe the observed islands, and kinetic models are necessary.

II. ENERGY OF A STRAINED VICINAL SURFACE

The energy of a vicinal surface per unit area is[24,25]

$$\gamma = \gamma_0 + \lambda |\theta|/h, \tag{1}$$

where γ_0 is surface tension of the singular crystal surface, θ is the slope of the surface with respect to the singular crystal orientation ($\theta = \tan \vartheta$, where ϑ is the angle between the vicinal and the singular surface), h is the height of the steps, and $\lambda(\theta)$ is the energy of a step per its unit length. The step energy $\lambda(\theta)$ consists of the energy λ_0 of an isolated step and the energy of the step-step interaction. The latter quantity originates from the elastic dipole-dipole interaction between steps and is proportional to θ^2, so that

$$\lambda = \lambda_0 + 2\lambda_d \theta^2. \tag{2}$$

Here λ_d is a constant and the factor of 2 is introduced to keep the same notation as in Refs. 16 and 26.

Xie *et al.*[16] found, by means of atomistic calculations of the step energies on a strained Si(001) surface, that the strain strongly influences the line energy of an isolated step λ_0. Specifically, a 2% strain changes the step energies by 150 meV per ledge atom, a quantity which is large compared to the energies of these steps on an unstrained surface. Moreover, the effect has opposite signs for compressive and tensile strain, respectively decreasing or increasing the step energy by the mentioned quantity.

Let us show now that this effect can be explained very generally as an interaction between the step strain field and the uniform strain field of compression or tension. The interaction energy of two strain fields, 1 and 2, can be written as (Ref. 27, Sec. 12.1)

$$U = -\int \mathbf{f}^{(1)}(\mathbf{r}) \cdot \mathbf{u}^{(2)}(\mathbf{r}) d^2 r, \tag{3}$$

where $\mathbf{f}^{(1)}(\mathbf{r})$ is the surface force field producing the strain field 1 and $\mathbf{u}^{(2)}(\mathbf{r})$ is the displacement field 2. The integral is taken over the flat surface of the crystal.

The strain field 1 is that of a surface step. The force $\mathbf{f}^{(1)}(\mathbf{r})$ arises from the interaction forces between atoms near the step edge. At distances away from the step that are large compared to the lattice spacing, the displacement field produced by this force distribution can be described by a multipole expansion, similarly to the corresponding problem in electrostatics. The displacement vector in elasticity requires higher order tensors than the scalar potential in electrostatics, so that the elastic dipole is a second-rank tensor (Ref. 27, Sec. 22). The strain field of a straight step can be described by two components of an elastic dipole.[28,29] The dipole force has a component normal to the surface, $f_z = Q_z \partial \delta(x)/\partial x$, due to the uncompensated moment of the surface stress, and a component in the surface plane, $f_x = Q_x \partial \delta(x)/\partial x$, which is a property of any linear crystal defect. Here, x is the coordinate in the surface plane in the direction normal to the step line and z is the coordinate normal to the surface. We do not combine the two components of the force into a vector, since Q_x and Q_z do not form a vector (rather, they are two components of the second-rank tensor). Numerical values of the coefficients Q_x, Q_z can be obtained from atomistic simulations of the steps on various surfaces of semiconductors and metals.[26,30,31] Below we use the results[26] of atomistic calculations of the step-step interactions on Si(001) to estimate the dipole strength.

We consider a heteroepitaxial strained film and take as the strain field 2 the uniform strain due to a misfit ε_0 between the film and the substrate crystal, so that $u_x^{(2)} = -\varepsilon_0 x$. A larger lattice parameter of the film compared to that of the substrate, $\varepsilon_0 > 0$, gives rise to compressive strain in the film, which explains the minus sign in the expression above. Making the integral (3) by parts, we obtain the energy per unit length of the step

$$\lambda_s = Q_x \partial u_x^{(2)}/\partial x + Q_z \partial u_z^{(2)}/\partial x. \tag{4}$$

We restrict ourselves to sufficiently high elastic symmetry, so that the shear distortion $\partial u_z^{(2)}/\partial x$ is absent. In particular, the elastically isotropic case and the (001) surface orientation of a cubic crystal belong to this class. Then, we obtain a remarkably simple expression for the step energy change due

to its interaction with the uniform strain field of the misfit ε_0, which we denote λ_s (keeping λ_0 for the step energy on an unstrained surface),

$$\lambda_s = -Q_x \varepsilon_0 . \tag{5}$$

Equation (5) explains the result of the atomistic calculations[16] which showed that the change of the step energy by an external strain field is proportional to the strain ε_0. It follows also that λ_s is proportional to the dipole strength of the step Q_x, the quantity which is responsible for the step-step repulsion on an unstrained surface. The interaction energy of two parallel steps separated by the distance x is, per unit step length,[28,29]

$$U(x) = \frac{2(1-\nu^2)(Q_x^2 \pm Q_z^2)}{\pi Y x^2}, \tag{6}$$

where Y is the Young modulus and ν is the Poisson ratio. We restrict ourselves to the elastic isotropy. The two signs correspond to two steps of the same sense (both up or both down) versus two steps of the opposite sense (one up and one down), respectively. The atomistic calculations of the step energies on an unstrained Si(001) surface[26] show that the interaction energies for pairs of steps of the same and of opposite senses differ by not more than 12%. We conclude that $Q_x \gg Q_z$ and use this assumption to simplify our formulas. We checked the effect of Q_z and did not find any qualitative changes in the results. Then, applying Eq. (6) to a vicinal surface with miscut $\theta = h/x$ and taking into account only the interactions between nearest-neighbor steps, we obtain by comparing Eqs. (2) and (6):

$$\lambda_d = \frac{(1-\nu^2)Q^2}{\pi Y h^2}. \tag{7}$$

Here, Q is written instead of Q_x for simplicity.

We can determine Q for different types of steps on the unstrained Si(001) surface using the values of λ_d obtained in the atomistic calculations.[26] We use the surface lattice constant $a = 3.85$ Å as a natural length unit and the elastic constants[26] $Y = 63.1$ eV/a^3 and $\nu = 0.333$. The 2×1 reconstruction of the Si(001) surface gives rise to either alternating S_A and S_B steps of single-atomic-layer height $h = a/\sqrt{8}$, which bound 90° domains with different orientation of the reconstruction, or double-layer steps D_A and D_B.[32] The calculations[26] yield a vanishingly small dipole-dipole interaction λ_d between S_A steps. Then, according to Eq. (5), the influence of strain on the energy of this step is also negligible, and this is confirmed by the calculation of the S_A step energy on a strained surface.[16]

Considering the S_B steps, we take into account that the distance between these steps is twice the distance between the neighboring steps (which are S_A and S_B), so that a factor of 1/4 should be introduced in the right-hand sides of Eqs. (6) and (7). With the value[26] $\lambda_d = 0.728$ eV/a we obtain, from Eq. (7), $Q = 8.95$ eV/a for S_B steps. The double-layer height steps D_B are separated by twice the distance between steps, to maintain the same miscut angle,[26] which results in an additional factor of 4 in Eq. (7). With the value $\lambda_d = 1.271$ eV/a we obtain $Q = 5.92$ eV/a for D_B steps.

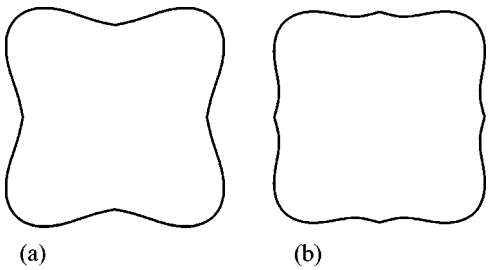

FIG. 1. Qualitative polar plots of surface energy for (a) an unstrained and (b) a strained crystal.

Now, with the misfit $\varepsilon_0 = 0.02$ used in the atomistic calculations[16] we obtain from Eq. (5) $\lambda_s = -180$ meV/a and -120 meV/a for S_B and D_B steps, respectively. These values agree well with the ones obtained by Xie *et al.*,[16] approximately -150 meV/a for both steps, with a somewhat larger value for the S_B step. This agreement confirms our interpretation of the influence of the uniform strain on the energy of an isolated step as an interaction between the strain field of the step and the uniform strain. The change of the step energy under the action of the strain λ_s is large compared to the step energy on an unstrained surface λ_0, which is -11 and -42 meV/a for S_B and D_B steps, respectively.[26] Below we neglect λ_0 compared to λ_s, with the aim to simplify formulas. This assumption does not significantly alter the results and λ_0 can be easily reintroduced in the equations if necessary.

Thus, the step energy on a strained vicinal surface is

$$\lambda = \lambda_s + 2\lambda_d \theta^2, \tag{8}$$

where the line energy of an isolated step λ_s, given by Eq. (5), is proportional to the strain ε_0 and can be either positive or negative, depending on the sign of the strain. For $Q_x > 0$, compressive strain gives rise to a negative λ_s; see Eq. (5). For sufficiently small miscut angles θ, the surface energy of a vicinal surface is lower than the energy of the singular facet. The minima of the surface energy (1) are obtained at

$$\theta_0 = \pm(|\lambda_s|/6\lambda_d)^{1/2}. \tag{9}$$

With the values discussed above, we obtain (for the misfit $\varepsilon_0 = 0.04$ of Ge/Si) the minima of the surface energy at the miscut angles $\vartheta_0 = \arctan\theta_0$ equal to $\pm 4.8°$ for S_B steps and $\pm 1.8°$ for D_B steps.

The analysis above shows that the presence of compressive strain (for $Q_x > 0$) qualitatively changes the azimuthal dependence of the crystal surface energy. The cusp at the singular orientation of the surface turns from a minimum to a local maximum of the surface energy, while the minimum is achieved at an angle which scales as $\varepsilon_0^{1/2}$ and typically makes a few degrees with the singular orientation. Figure 1 presents a qualitative picture of these changes.

For unstrained crystals, knowledge of the orientational dependence of the surface energy is sufficient to determine the equilibrium crystal shape by means of the Wulff construction. In contrast, the shape transformation of a strained crys-

tal influences its elastic energy. In particular, the energy of a singular facet can be decreased by development of surface undulations that both decrease the elastic energy and increase the number of steps with negative line energy. The growth of the undulations is limited by the short-range step-step repulsion which makes small distances between steps unfavorable. The balance between all these contributions and their influence on the energy of an undulated crystal surface is considered in the next section.

III. MORPHOLOGICAL INSTABILITY OF A STRAINED CRYSTAL BELOW THE ROUGHENING TRANSITION

The morphological instability of strained solids *above* the roughening transition has already been studied in detail.[33–38,13] The origin of the instability is regarded as a competition between the elastic energy release by surface undulations and the respective surface area increase. The surface tension of the solid is taken independent of orientation, an approximation which is valid above the roughening transition. The competing energy contributions result in a critical wavelength of the undulations: all modes with wavelengths exceeding the critical one are unstable and get amplified.

The morphological instability of a strained crystal *below* the roughening transition is qualitatively different, since the crystal surface consists of steps and terraces and the surface energy strongly depends on the surface orientation, as discussed in the previous section. It also follows from the previous section that the line energy of steps becomes negative under compressive strain and hence favors undulations, in addition to the elastic relaxation. Our aim now is to calculate the energy of the periodically undulated surface of a strained crystal. We restrict ourselves to a surface consisting of facets formed by equidistantly spaced steps and do not search for an optimum shape of the undulation. We consider only the energetics and do not study surface kinetics, a problem which is fairly complicated even in the absence of strain.[22,39,40] We have proposed a kinetic model for a single undulation in a previous publication[20] and further develop this kinetic model in Sec. VIII to describe the kinetics of a single three-dimensional strained island.

The action of the bulk stress on the step edge produces, in addition to the force dipole described above, an uncompensated force, a force monopole[41] $f_x(x)=P\delta(x)$, where $P=\pm h\sigma_{xx}$. The x axis is in the surface plane and directed normal to the step line, h is the step height, σ_{xx} is the in-plane bulk stress at the step location, and the plus sign corresponds to an upward step and the minus to a step down. The displacement field of the surface step can be evaluated using the general formula

$$u_i(\mathbf{r})=\int_{-\infty}^{\infty} G_{ij}(\mathbf{r}-\mathbf{r}')f_j(\mathbf{r}')d^2r', \tag{10}$$

where $G_{ij}(\mathbf{r})$ is the ith component of displacement at the surface due to a unit force applied to the surface in the jth direction. The coordinate y is along the step edge. Using the expressions for the elastic Green function $G_{ij}(\mathbf{r})$ for a semi-infinite elastically isotropic solid[42] and calculating the integrals with the δ function, we obtain

$$u_x(x)=-\frac{2(1-\nu^2)}{\pi Y}\left(P+Q\frac{\partial}{\partial x}\right)\ln|x|, \tag{11}$$

where we have neglected Q_z in comparison with $Q_x\approx Q$, as discussed above.

The elastic interaction energy V_{nm} per unit step length of two parallel steps separated by a distance $x=x_n-x_m$ is obtained by using Eq. (3):

$$V_{nm}=\frac{2(1-\nu^2)}{\pi Y}[P_mP_n+(P_n-P_m)Q\partial/\partial x - Q^2\partial^2/\partial x^2]\ln|x|. \tag{12}$$

Here, $P_n=s_nh\sigma_{xx}$, where $s_n=+1$ for a step up and $s_n=-1$ for a step down.

The first term of Eq. (12) gives, after summing over the steps, the elastic relaxation energy in the small-slope approximation.[3–5,12,13] The second term, the monopole-dipole interaction, is present only if the interacting steps have different monopole strengths. In the problem considered in this section, the monopole-dipole interaction takes place between a step up and a step down. It is absent for steps on a strained vicinal surface.[41] The monopole-dipole interaction between steps of the same sense is also present, as discussed in the next sections, if the bulk stress (and hence the monopole strength) is influenced by the stress fields of other steps forming a strained island. The last term of Eq. (12) describes the step-step repulsion in the absence of strain and coincides with Eq. (6), where Q_z is neglected compared to Q_x.

The ratio of the dipole to monopole strengths is the characteristic length of the problem:

$$l_0=Q/|P|. \tag{13}$$

Using the values for the Ge/Si(001) system discussed above, we find $l_0=3.3a$ for S_B steps and $l_0=2.2a$ for D_B steps. Hence, l_0 amounts to a few times the surface unit cell parameter a.

The ratio h/l_0 is the only dimensionless free parameter of the problem under consideration. One has $l_0\propto\varepsilon_0^{-1}$ and hence $h/l_0\propto\varepsilon_0$. We employ throughout the paper the small-slope approximation which consists in replacing the surface steps by force multipoles applied to a flat surface. We will see below that the surface slopes of the ridges and islands are of the order of h/l_0. Hence, applicability of the present theory requires $h/l_0\ll 1$. With the values given above, we find $h/l_0=0.1$ and 0.3 for S_B and D_B steps in the Ge/Si(001) system, respectively. A 4% misfit of the Ge/Si is therefore at the upper limit of applicability of the present theory. In other words, we expect that the small-slope approximation is still valid for the slope of $11°(=0.2$ rad) of the Ge/Si(001) pyramidal islands.

We can also express the slope θ_0 of the vicinal surface corresponding to a minimum of the surface energy, Eq. (9), through l_0. Using the expressions for λ_s and λ_d, Eqs. (5) and (7), we obtain

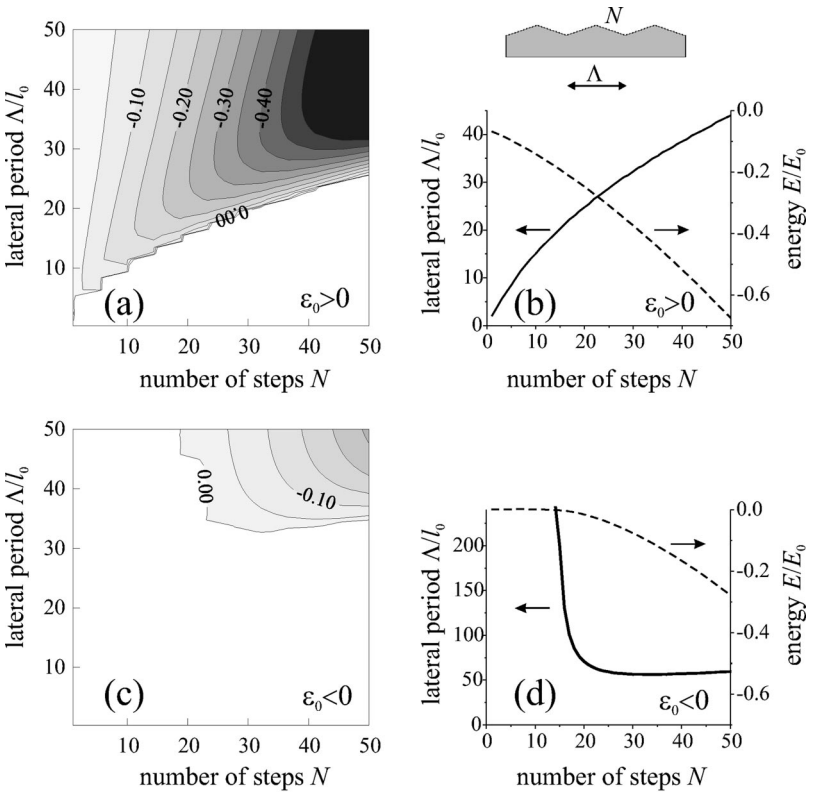

FIG. 2. The energy release per unit surface area of a laterally strained crystal developing periodic undulations. (a),(b) Compressive and (c),(d) tensile strain. Left column: the energy distribution plotted vs the undulation period Λ (measured in units of l_0) and height (measured in number of steps, N). The regions of negative energy (with respect to the flat surface) are only shown. Right column: the energy minimum and the corresponding lateral period for a given undulation height. $h/l_0=0.1$.

$$\theta_0=\pm\left(\frac{\pi}{6(1+\nu)}\frac{h}{l_0}\right)^{1/2}. \tag{14}$$

We now consider the periodically undulated stepped surface of a laterally strained crystal, which is formed by N equidistant steps up followed by N steps down. The distance between steps $\Lambda/(2N)$, where Λ is the undulation period, can be varied and hence the orientation of the ''facets'' formed by the steps is arbitrary. The energy of the undulations with respect to the flat strained surface consists of the line energies of the steps (5) and the energy of step-step interaction obtained by summation of the terms V_{nm}. Using the definition of l_0, Eq. (13), we find for the undulation energy per unit area of the flat surface

$$E=E_0\frac{2h^2}{\Lambda}\left\{\frac{2(1+\nu)}{\pi}{\sum_{mn}}'\left[s_m s_n\ln|x_m-x_n|+\frac{l_0^2}{(x_m-x_n)^2}\right]-\frac{l_0}{h}N\right\}. \tag{15}$$

Here $E_0=Y\varepsilon_0^2/(1-\nu)$ is the elastic energy density of a uniformly strained crystal with flat surface due to the in-plane strain ε_0. The sum over m runs over all steps, while the sum over n runs over N steps of a single ''facet,'' e.g., $0<x_n<\Lambda/2$. The prime at the sum indicates that the term $m=n$ is excluded from the summation. The monopole-dipole interaction vanishes after summation over the steps, due to mirror symmetry of the step distribution. The convergence of the sum of logarithmic terms in Eq. (15) is obtained by performing first summation over a distant period plus the symmetrically located one. The contribution decays as the square of the distance. The minus sign of the last term in Eq. (15) (i.e., $-Nl_0/h$) corresponds to compressive strain and the negative line energy of steps. For tensile strain, this term has the opposite sign.

Figures 2(a) and 2(c) presents the results of numerical calculations of the undulation energy density (15) as a function of the undulation period Λ and the number of steps per facet, N. The energy density E is expressed in units of the elastic energy density E_0 of a uniformly strained crystal. In the case of compressive strain, there is no energetic barrier for surface undulations: the energy continuously decreases as the undulations grow. The initial single-step height undulation ($N=1$, a periodic sequence of up and down steps) decreases the energy for $\Lambda/l_0>1.1$; the energy minimum is achieved at $\Lambda/l_0\approx 2$. The energetically favorable growth route, Fig. 2(b), consists in a simultaneous increase of the undulation period Λ and the number of steps, N, in it. Approximating the dependence $\Lambda(N)$ by a straight line $\Lambda/l_0\approx N$, we find that the facet slope is roughly constant, $\theta=2Nh/\Lambda=2h/l_0$. However, the variation of the period with increasing height can be kinetically hindered.[43,44]

In the case of tensile strain, the line energy of steps is positive and the competition between the released elastic energy and the increased surface energy is similar to the one causing the morphological instability above the roughening transition.[33–38,13] Figure 2(d) shows that, although an instability is formally present for any N, undulations with a height smaller than about $20h$ possess very large periods and give rise to only an insignificant energy gain.

In the following sections, we generalize the energetics of straight steps presented above and our kinetic model of Ref.

20 to three-dimensional islands (Stranski-Krastanov growth). We consider axially symmetric islands with the surface consisting of circular steps whose line energy (5) is assumed to be constant along the step. However, the line energies of different steps may differ since the bulk strain acting on them is produced not only by the misfit but also by other steps. The strain relaxation at the island top and the strain concentration at the island base respectively decrease or increase the line energy.

IV. STRAIN AND STRESS PRODUCED BY A THREE-DIMENSIONAL ISLAND

We proceed now to the energetics of three-dimensional strained islands and restrict ourselves to axially symmetric islands whose surface is formed by coaxial circular steps. Let us first determine the displacement field of a single circular step on a strained surface and then obtain, by summing over the steps, the strain and stress fields of a three-dimensional island.

The elastic field of a step of radius r_n on a strained surface is that of the axially symmetric distribution of force monopoles $f_r(r)=P\delta(r-r_n)$ and force dipoles $f_r(r)=Q\partial\delta(r-r_n)/\partial r$. Here r is the radial coordinate, h is the step height, $P=-h\sigma_{rr}$, and σ_{rr} is the in-plane bulk stress at the step location acting normal to the step line. The minus sign corresponds to downward steps and gives rise to a positive monopole P for compressive bulk stress ($\sigma_{rr}<0$). Evaluation of the integrals (10) in polar coordinates gives the displacement field of a circular step of radius r_n:

$$u_r(r)=\frac{1-\nu^2}{\pi Y}(P_n-Q\partial/\partial r_n)W(r/r_n), \tag{16}$$

where P_n is the monopole strength of the nth step. Below we take into account that the value of P_n is influenced by the stress produced by other steps. It is assumed that the dipole strength is not changed under the action of strain.

We have denoted

$$W(\rho)\equiv\int_0^{2\pi}\frac{\cos\varphi d\varphi}{\sqrt{1-2\rho\cos\varphi+\rho^2}}. \tag{17}$$

The integral (17) is elliptic and can be expressed via canonical elliptic integrals. However, we found the direct numerical evaluation more appropriate. In the limit $|r-r_n|\ll r,r_n$ one can expand $\cos\varphi\approx 1-\varphi^2/2$ in the denominator and obtain

$$W(r/r_n)\approx 2\ln(r_n/|r-r_n|), \tag{18}$$

so that the expression for the displacement field of a circular step (16) reduces to that of a straight step (11).

The radial strain $\delta\varepsilon_{rr}(r)=\partial u_r/\partial r$ due to the mth step is obtained by differentiating Eq. (16). We substitute the zeroth order approximation $P_0=-h\sigma_0$, where $\sigma_0=-Y\varepsilon_0/(1-\nu)$ is the stress produced by the uniform strain, and obtain

$$\delta\varepsilon_{rr}(r)=-\frac{1+\nu}{\pi}h\partial/\partial r[1-l_0\partial/\partial r_m]W(r/r_m), \tag{19}$$

where the length l_0 has been introduced by Eq. (13).

The two terms in the square brackets in Eq. (19) correspond to the monopole and quadrupole terms, respectively. Their ratio is of the order R/l_0, where R is the island base radius, so that the latter term can be neglected for reasonable island sizes which are much larger than a. Therefore, we take into account only the long-range term related to the monopole and obtain, by summation over all steps, the bulk strain at the position of the nth step $r=r_n$,

$$\varepsilon_n=\varepsilon_0\left[1-\frac{1+\nu}{\pi}h{\sum_m}'\frac{\partial W(r_n/r_m)}{\partial r_n}\right], \tag{20}$$

where, in the same way as above, the prime at the sum indicates that the term $m=n$ is not included in the summation.

Evaluation of the stress requires the determination of the normal strain $\varepsilon_{zz}\equiv\partial u_z/\partial z$. It can be found by employing the elastic Green tensor[42] for the bulk displacement field, rather than the surface one:

$$\varepsilon_{zz}(\mathbf{r})=\int_{-\infty}^{\infty}\partial G_{zj}(\mathbf{r}-\mathbf{r}')/\partial z|_{z=0}f_j(\mathbf{r}')d^2r',$$

where summation over $j=1,2$ is implied. Evaluation of the integral gives the normal strain at the surface caused by the nth step:

$$\varepsilon_{zz}(r)=-\frac{\nu(1+\nu)}{\pi Y}P_0(\partial/\partial r+1/r)W(r/r_n). \tag{21}$$

Using Eq. (16), we find the in-plane stress produced by a step of radius r_n:

$$\delta\sigma_{rr}=\frac{Y}{(1+\nu)(1-2\nu)}\left[(1-\nu)\frac{\partial u_r}{\partial r}+\nu\frac{u_r}{r}+\nu\varepsilon_{zz}\right]$$
$$=(P_0/\pi)(\partial/\partial r+\nu/r)W(r/r_n). \tag{22}$$

Summation of the stress produced by all steps gives the monopole strength of the nth step:

$$P_n/P_0=1-(h/\pi){\sum_m}'(\partial/\partial r_n+\nu/r_n)W(r_n/r_m). \tag{23}$$

The continuous limit of the equations above can be obtained by substituting $h\to\theta(r)dr$, where $\theta(r)=dz/dr$ is the local slope of the island surface $z(r)$, and replacing the sums by integrals. The rr component of the in-plane bulk strain at the island surface is obtained from Eq. (20):

$$\bar{\varepsilon}(r)=1-\frac{1+\nu}{\pi}\frac{\partial}{\partial r}\int_0^R\theta(r')W(r/r')dr', \tag{24}$$

where R is the island base radius and we have denoted $\bar{\varepsilon}(r)=\varepsilon_{rr}(r)/\varepsilon_0$. Hereafter we denote by overbars the dimensionless quantities of order unity. Similarly, the rr component of the bulk stress follows from Eq. (23):

$$\bar{\sigma}(r)=1-\frac{1}{\pi}\left(\frac{\partial}{\partial r}+\frac{\nu}{r}\right)\int_0^R\theta(r')W(r/r')dr', \tag{25}$$

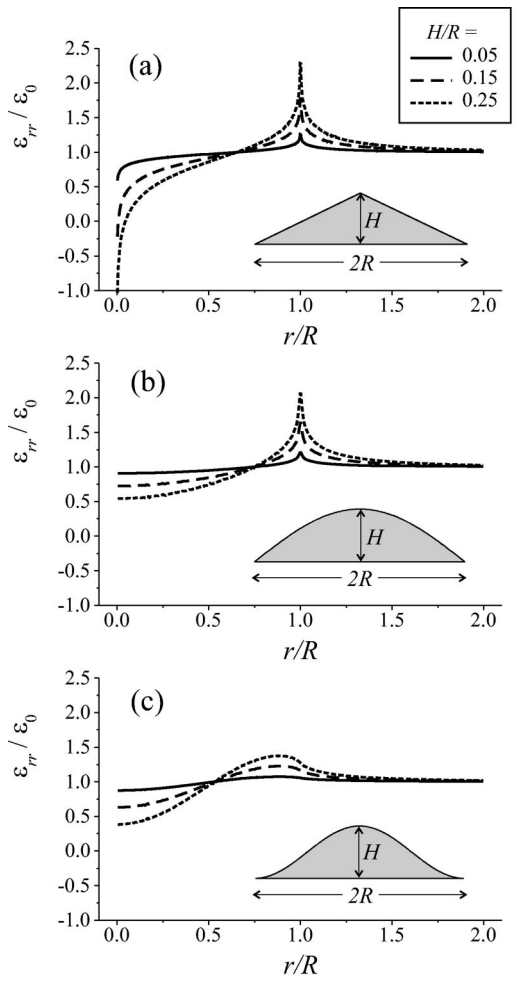

FIG. 3. Radial strain distributions at the surface of islands of different shapes calculated from Eq. (24). The insets show the island cross sections: (a) straight line, (b) half of a cosine period, and (c) full period of a cosine. Breaks in the island cross section give rise to strain singularities.

where $\bar{\sigma}(r)=\sigma_{rr}(r)/\sigma_0$. In the continuous limit, both the strain and the stress do not depend on the height of the individual steps and are solely determined by the island shape function $\theta(r)$.

Figure 3 presents the strain distributions calculated by Eq. (24) for islands of several model shapes. We consider axially symmetric islands generated by a straight line, half of a cosine period, and full period of a cosine. The island profile has breaks at the top and at the base in the first case, only at the base in the second case, and is smooth in the third case. We have chosen the same ratios of the island height H to its base $2R$. Strain relaxation at the island top and strain concentration at its base takes place in all three cases, in agreement with the finite-element calculations,[9] as well as other analytical[45] and numerical[46,47] calculations. It is also obvious from Fig. 3 that breaks in the island profile give rise to singularities of the strain. The smooth island profile [Fig. 3(c)] leads to smaller, although still pronounced, variations of strain.

Equations (24) and (25) provide a simple estimate of the strain and stress distributions for an arbitrary axially symmetric island in the small-slope approximation. This approximation replaces the island by forces applied to the flat surface. Hence, Eqs. (24), (25), and the strain distributions presented in Fig. 3 do not distinguish the strain at the island surface and that at the interface. An accurate determination of three-dimensional strain distribution, as well as the account of the island faceting, requires numerical finite-element calculations.[8–11]

V. ENERGY OF A STRAINED THREE-DIMENSIONAL ISLAND

The elastic interaction energy between two coaxial circular steps of radii r_n and r_m can be calculated using Eq. (3). Evaluating the integrals with δ functions, we obtain

$$U_{nm}=-\frac{2(1-\nu^2)}{Y}[P_mP_n-Q(P_n\partial/\partial r_m+P_m\partial/\partial r_n)+Q^2\partial^2/\partial r_m\partial r_n][r_nW(r_n/r_m)]. \tag{26}$$

In the limit $|r_m-r_n|\ll r_m,r_n$, the elastic interaction energy per unit step length, $V_{nm}=U_{nm}/(2\pi r_n)$, reduces to the interaction energy between two straight parallel steps given by Eq. (12). We note that if the variation of the monopole strength caused by strain fields of other steps is neglected, $P_m=P_n=P$, the monopole-dipole interaction between straight steps of the same sense is absent and only the monopole-monopole and dipole-dipole interactions are present.[41] However, the monopole-dipole interaction between two circular steps does not vanish even if the monopole strengths are equal, since the step radii differ.

Now we can write the energy of the island as

$$E=\sum_n L_n+\frac{1}{2}{\sum_{m,n}}' U_{nm}, \tag{27}$$

where

$$L_n=-2\pi r_nQ\varepsilon_n \tag{28}$$

is the line energy of the nth step. We consider the case of Stranski–Krastanov growth, with the substrate surface covered by a wetting layer. The surface tension of the wetting layer is the same as on the terraces of the island surface. The difference of the island energy from the flat layer energy is due to the step line energy and the step-step interaction energy, Eq. (27).

We apply the same substitution as above, $h\rightarrow\theta(r)dr$, to obtain the island energy in the continuous limit. Then, the line energy of the steps given by the first term of Eq. (27) becomes

$$\mathcal{L}=-2\pi Q\varepsilon_0h^{-1}\int_0^R\theta(r)\bar{\varepsilon}(r)rdr. \tag{29}$$

The step-step interaction energy in Eq. (27) consists of three terms given by Eq. (26), which are monopole-monopole, monopole-dipole, and dipole-dipole interactions.

We consider them separately. Going to the continuous limit of the first term in Eq. (26), we arrive at the monopole-monopole interaction energy

$$\mathcal{U}_{\rm mm} = -(1+\nu)E_0 \times \int\int_0^R \theta(r)\,\theta(r')\,\overline{\sigma}(r)\,\overline{\sigma}(r')\,rW(r/r')\,dr\,dr', \tag{30}$$

where $E_0 = Y\varepsilon_0^2/(1-\nu)$ is the elastic energy density of the uniform strained film, as introduced in Sec. III. In deriving Eq. (30), we took into account that $P_0 = -h\sigma_0 = hY\varepsilon_0/(1-\nu)$. The symmetry of the integrand with respect to its two arguments is ensured by the identity $rW(r/r') = r'W(r'/r)$ which follows from the definition of $W(r/r')$ in Eq. (17). The monopole-monopole interaction energy is obviously nothing else but the elastic relaxation energy in the small-slope approximation.[3–5,12,13]

A similar treatment of the monopole-dipole interaction given by the second term of Eq. (26) leads to

$$\mathcal{U}_{\rm md} = (1+\nu)E_0 l_0 \int\int_0^R \theta(r)\,\theta(r')\,[\overline{\sigma}(r)\,\partial/\partial r' + \overline{\sigma}(r')\,\partial/\partial r]\,rW(r/r')\,dr\,dr', \tag{31}$$

where the characteristic length of the problem l_0 has been introduced by Eq. (20).

The dipole-dipole interaction cannot be treated similarly to the monopole-monopole and monopole-dipole terms above, since the corresponding integral diverges at $r = r'$. The behavior of the integral at $r \to r'$ can be established using Eq. (18), which gives $\partial^2 W(r/r')/\partial r\,\partial r' = -2/(r-r')^2$ for $|r-r'| \ll r, r'$. The integral diverges even if treated as a principal value. To make it meaningful, we take into account that the nearest steps are separated by the distance $h/\theta(r)$. Then, a finite interval $-h/\xi_{\rm dd}\theta(r) < r - r' < h/\xi_{\rm dd}\theta(r)$, where $\xi_{\rm dd}$ is a constant of the order of unity, should be excluded from the integration range. We find below, by comparing with numerical calculations, that $\xi_{\rm dd} \approx 1.4$. Since the integral is acquired around $r \approx r'$, the approximation (18) is applicable and the integration gives

$$\mathcal{U}_{\rm dd} = 4(1+\nu)\xi_{\rm dd}E_0 l_0^2 h^{-1} \int_0^R r\,\theta^3(r)\,dr. \tag{32}$$

The sum $E = \mathcal{L} + \mathcal{U}_{\rm mm} + \mathcal{U}_{\rm md} + \mathcal{U}_{\rm dd}$ gives the energy of the island of arbitrary shape $\theta(r)$. In principle, the shape of an island which minimizes the energy can be found by varying the energy with respect to $\theta(r)$ under additional restrictions, e.g., fixed volume or height of the island. However, such a minimization leads to nonlinear integro-differential equations. On the other hand, the energy E derived above does not imply faceting of the island surface, which is an additional effect governed by the surface reconstruction energies. We mimic faceting of the island by restricting its profile $z(r)$ to be a linear or piecewise linear function. The former case can be investigated analytically, if we also neglect the variation of the strain ε_{rr} and the stress σ_{rr}. This is done in the next section. Islands consisting of two ''facets'' are analyzed in Sec. VII.

VI. ISLANDS WITH CONSTANT SURFACE SLOPE

Let us determine the energy of a cone-shaped island, the slope θ of which is constant. Such a cone is an axially symmetric analog of the pyramidal islands investigated by Tersoff *et al.*[3] Let us first neglect the influence of step strain fields on other steps, i.e., take $\overline{\varepsilon}(r) = 1$ and $\overline{\sigma}(r) = 1$. Then, the integrals (29)–(32) can be evaluated analytically and yield the energy of a strained island,

$$E = (1+\nu)E_0 l_0^3 (\Gamma \overline{v}^{2/3}\theta^{1/3} - \xi_{\rm mm}\overline{v}\,\theta), \tag{33}$$

where we have denoted

$$\Gamma = -\frac{\pi}{1+\nu} + \xi_{\rm md}\theta + 2\xi_{\rm dd}\theta^2 l_0/h. \tag{34}$$

We have expressed the island energy E through the dimensionless volume $\overline{v} = \pi R^3\theta/3l_0^3$ and omitted the factor $\pi/3$ to simplify the formulas. The constant factors entering Eqs. (33) and (34) are

$$\xi_{\rm mm} \equiv \int\int_0^1 \rho W(\rho/\rho')\,d\rho\,d\rho' \approx 1.11, \tag{35}$$

$$\xi_{\rm md} \equiv 2\int_0^1 \rho W(\rho)\,d\rho \approx 3.33, \tag{36}$$

and $\xi_{\rm dd} \approx 1.4$ as described below.

Equation (33) represents the island energy in the same form as given by Tersoff *et al.*:[3] the first term is the surface energy proportional to $v^{2/3}$ and the second term is the elastic energy proportional to v. In contrast to Ref. 3, where both Γ and θ were treated as constants corresponding to a cusp in the polar plot of the surface energy and Γ was strictly positive, our analysis of vicinal surfaces led us to the surface energy (34) which depends on the slope θ and is negative for small θ.

Now, we search for a minimum of the island energy (33) over θ for a given volume v. The only free parameter of the problem is the ratio h/l_0, which is proportional to the misfit ε_0.

Figure 4 compares the energies obtained by the analytical formulas (33) and (34) with the numerical calculation based on Eq. (27), where the constant slope is obtained by taking equidistant steps. We fixed the step height $h/l_0 = 0.1$ and the island volume $\overline{v} = 2.5 \times 10^3$ and calculated the energy E as a function of the slope θ. Different contributions to the energy are presented separately. We find a good agreement between numerical and analytical calculations for each term. We used the calculations of the dipole-dipole term to obtain $\xi_{\rm dd} \approx 1.4$. At $\theta \to 0$, the island energy is dominated by the negative line tension of steps and the elastic energy (the monopole-monopole interaction), which is also negative. At large θ, the distance between steps is smaller and the energy increases

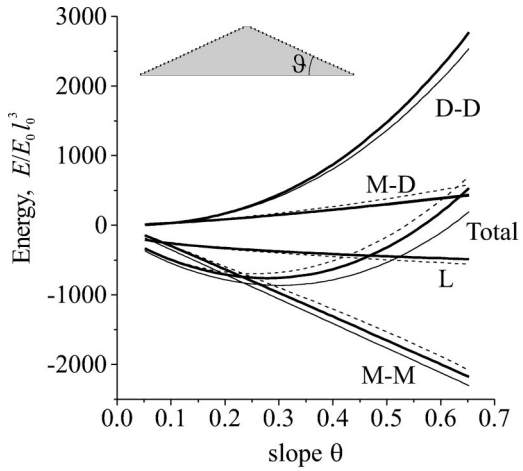

FIG. 4. Different contributions to the energy of a cone-shaped island as a function of its slope $\theta=\tan\vartheta$: L denotes the line energy of steps, M-M is the monopole-monopole interaction energy (elastic energy), M-D is the monopole-dipole interaction energy, D-D is the dipole-dipole interaction energy, and ''Total'' denotes the sum of all these contributions. Thick lines: numerical calculation of the step energies and step-step interactions with Eq. (27) taking $\epsilon_n/\epsilon_0=1$ and $\sigma_n/\sigma_0=1$; thin lines: analytical approximation (33); dashed lines: numerical calculation taking into account the variations of ϵ_n and σ_n.

due to the short-range repulsion between steps (the dipole-dipole interaction). The energy minimum is obtained at an intermediate value of θ.

The energy minimum for a given volume v of a cone-shaped island under compressive strain is presented in Fig. 5 by line 1. For comparison, line $1'$ shows its energy under tensile strain. It is obtained by inverting the signs of the first two terms in Eq. (34). Other lines in the figure are described in the next sections. We find that, under compressive strain, the island energy monotonously decreases with increasing

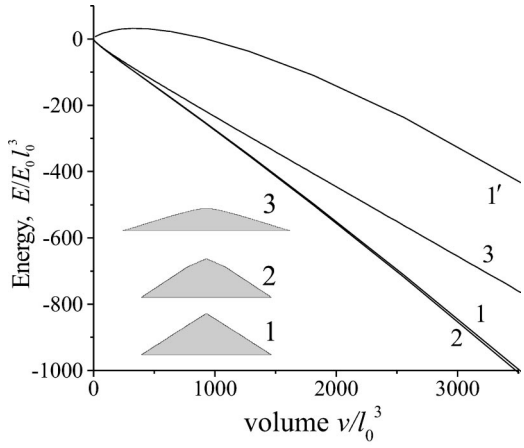

FIG. 5. Island energies as functions of the island volume: 1: conical island with constant slope under compressive strain. $1'$: the same island under tensile strain. 2: island with two ''facets'' of different slopes. 3: island obtained by the kinetic model described in Sec. VIII. Insets show cross sections of the islands of volume $v/l_0^3=3500$ in a common scale. The step height is $h=0.1l_0$.

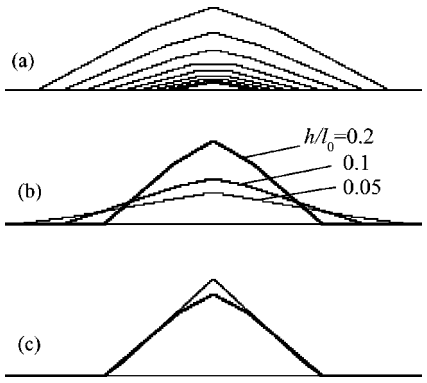

FIG. 6. Shapes of strained islands with two facets: (a) variation of shape with increasing volume, volumes of subsequent islands differ by a factor of 2, $h/l_0=0.2$; (b) shapes of islands with the same volume $v=6.4\times10^5h^3$ for different ratios h/l_0; (c) shape of the island obtained by energy minimization taking into account variations of ϵ_n and σ_n (thick line) and under the additional assumption that $\epsilon_n=\epsilon_0, \sigma_n=\sigma_0$ (thin line), $h/l_0=0.2$.

island volume. Hence, there is no *energetic* barrier for the island to grow. Below (Sec. VIII) we find a *kinetic* barrier for the island nucleation. Tensile strain gives rise to an energy barrier which needs to be overcome before the island can grow, as discussed in Refs. 3, 10 and 48. For the value $h=0.1l_0$ used in Fig. 5, the barrier $E\approx32E_0l_0^3$ is reached at $v\approx320l_0^3$. With the parameter estimates given above and taking $l_0=2.5a$, we obtain a barrier height of 75 eV, and a fluctuation which would overcome this barrier should involve some thousands of atoms. Such a fluctuation is highly unlikely, which explains the differences in the growths of compressive and tensile heteroepitaxial layers.[16] Our estimate of the barrier height is much larger than the estimates of Refs. 10 and 48 since we use the line energy of a step on a strained crystal surface[16] which is large compared to typical step energies on an unstrained surface used in the other estimates.

VII. ISLANDS WITH TWO "FACETS"

We now relax the restriction of a constant slope on the island surface and allow the presence of two different slopes. The slopes and the sizes of corresponding ''facets'' are arbitrary and are found by minimizing the island energy with respect to these parameters at a given volume. We even allow the ''facets'' consisting of one step. In the latter case, the separations between all but one steps are equal. Figure 6(a) compares the island shapes obtained by energy minimization for $h/l_0=0.2$. The volumes of the islands differ by a factor of 2. We find that the surface slope at the island bottom continuously increases as the volume is increased. The top ''facet'' is flat at small volumes and possesses a relatively small slope at larger volumes.

Figure 6(b) compares the island shapes for different ratios of h/l_0. We vary the misfit ε_0 while all other parameters of the system remain constant. Hence, the ratio h/l_0 is proportional to ε_0. The island volume v is constant, so that the dimensionless volume $\bar{v}$ varies as l_0^{-3}. One can see from Fig.

6(b) that the island shape strongly depends on h/l_0. When h/l_0 increases, the surface slope increases and the surface breaks into two facets with noticeably different slopes. The top part of the island is flatter and the bottom is steeper.

Line 2 in Fig. 5 presents the volume dependence of the energy of the two-facet island. Comparison with line 1 presenting the energy of the single-facet island shows that the appearance of the second facet gives rise to very little gain in the island energy.

The presence of the second facet is due to strain relaxation in the top part of the island. This is demonstrated by Fig. 6(c) where the shape of the island obtained by minimizing the energy is compared with the one obtained by neglecting the variation of ε_n and σ_n, i.e., by taking $\varepsilon_n=\varepsilon_0$ and $\sigma_n=\sigma_0$. In the latter case, the top facet with a smaller slope does not develop.

VIII. GROWTH KINETICS OF STRAINED ISLANDS

In this section, we propose a model of the island growth kinetics. It is an extension of our preliminary one-dimensional model with straight steps[20] to the two-dimensional case of circular steps and is based on the island energies derived above. We assume that the Stranski-Krastanov growth of strained islands proceeds by attachment of adatoms from the flat wetting layer. Attachment of adatoms to a step from the lower terrace and detachment to the higher terrace provides an adatom flux to the island apex. We assume that a new two-dimensional island is nucleated on the top of the three-dimensional island as soon as the step edge of the newly created island expands after it is created. We neglect the incoming flux of atoms and assume that the three-dimensional island is fed solely by adatoms from the flat surface of the wetting layer. The adatom concentration far from the island is taken equal to the equilibrium adatom concentration. In this model, the incoming atomic flux increases the adatom concentration and gives rise to the nucleation of other three-dimensional islands far from the island under consideration. These islands serve as sinks for atoms from the deposition flux. The island nucleation reduces the adatom concentration to the equilibrium concentration. Any other possible interaction between the islands is neglected.

We follow the familiar Burton-Cabrera-Frank step kinetics equations[21–23] with the appropriate modification for circular steps.[18,19] The adatom density $c(r)$ on a terrace between two steps satisfies the continuity equation

$$\frac{\partial c}{\partial t}=-\nabla\cdot\mathbf{J}, \tag{37}$$

where $\mathbf{J}(r)$ is the adatom current along the surface. We do not include the deposition flux into the continuity equation, as discussed above. We make the common assumption that the step motion is slow compared to the equilibration of the adatom distribution and take $\partial c/\partial t=0$. Then, the continuity equation (37) can be written in polar coordinates as

$$\frac{dJ_r}{dr}+\frac{J_r}{r}=0, \tag{38}$$

where $J_r(r)$ is the radial component of the current $\mathbf{J}(r)$. Solution of this equation on the nth terrace, $r_n<r<r_{n+1}$, where r_n is the radius of the nth step, is $J_r(r)=j_n/r$, where j_n is a constant. On the top terrace $n=1$, one has $j_1=0$. The step moves due to the difference between the adatom currents from two adjacent terraces and hence its velocity is $dr_n/dt=-\mathcal{S}(J_n-J_{n-1})$, where $\mathcal{S}$ is the surface area per atom in the solid phase. With the currents obtained above, we have

$$dr_n/dt=-\mathcal{S}(j_n-j_{n-1})/r_n. \tag{39}$$

The current $\mathbf{J}(r)$ is given by Fick's law

$$\mathbf{J}=-D_s\nabla c, \tag{40}$$

where D_s is the surface diffusion coefficient. The solution of this equation on the nth terrace is

$$c(r)=-(j_n/D_s)\ln(r/r_n)+a_n. \tag{41}$$

The constants j_n and a_n can be found from the common assumption that the adatom flux to the nth step is proportional to the difference between the adatom concentration at the step $c(r_n\pm 0)$ and the equilibrium adatom concentration at the step c_n:

$$K[c(r_n+0)-c_n]=-J(r_n+0), \tag{42}$$

$$K[c(r_{n+1}-0)-c_{n+1}]=J(r_{n+1}-0), \tag{43}$$

where K is a kinetic coefficient. The limit $K\to\infty$ is referred to as the case of diffusion-limited kinetics (the adatom concentration at a step is equal to the equilibrium concentration), while the opposite limit $K\to 0$ is the case of attachment-limited kinetics.

From these boundary conditions we find

$$j_n=-D_s\frac{c_{n+1}-c_n}{\ln(r_{n+1}/r_n)+l_K(r_{n+1}^{-1}+r_n^{-1})}, \tag{44}$$

where $l_K=D_s/K$. The equilibrium adatom concentration at nth step, c_n, can be expressed through the equilibrium adatom concentration at an isolated step c_0 and the chemical potential of the step μ_n: $c_n=c_0\exp(\mu_n/kT)$. Taking into account that $\mu_n/kT\ll 1$, one can expand $c_n\approx c_0(1+\mu_n/kT)$. Finally, the island kinetics are described by the following set of equations:

$$\frac{dr_n}{dt}=\frac{b}{r_n}\left[\frac{\mu_{n+1}-\mu_n}{\ln(r_{n+1}/r_n)+l_K(r_{n+1}^{-1}+r_n^{-1})}-\frac{\mu_n-\mu_{n-1}}{\ln(r_n/r_{n-1})+l_K(r_n^{-1}+r_{n-1}^{-1})}\right], \tag{45}$$

where $b=c_0D_s\mathcal{S}/kT$ is a constant. For the first(top) step, the second term of Eq. (45) is omitted. At the bottom of the island, one can virtually add one more circular step of a radius large compared with the island size. This step provides the equilibrium adatoms concentration at its location. Taking the limit $r_{N+1}\to\infty$, we find that the requirement of

the equilibrium adatom concentration at infinity is equivalent to omitting the first term in Eq. (45) for the bottom step.

The chemical potential of a step μ_n is the change of its energy when an atom is attached to it. The step is advanced and the energy of its elastic interaction with other steps changes. The change of area of the circular step by the atomic area $\mathcal{S}$ gives rise to a radius change $\Delta r_n = \mathcal{S}/(2\pi r_n)$. Then, the chemical potential is $\mu_n = (\delta E/\delta r_n)\Delta r_n$. Using Eqs. (27) and (28), we obtain

$$\mu_n = \mathcal{S}\left[-\frac{Q\varepsilon_n}{r_n} + \frac{1}{2\pi r_n} \sum_m{}' \frac{\partial U_{nm}}{\partial r_n} \right]. \tag{46}$$

The interaction energy of two circular steps on the strained surface is given by Eq. (26).

Equations (45) describe the kinetics of a set of circular steps. The chemical potential of the nth step μ_n, Eq. (46), is expressed through the strain ε_n, Eq. (20), acting on this step and the step-step interaction energy U_{nm}, Eq. (26), where, in turn, the monopole strength P_n of the nth step is given by Eq. (23). Previous investigations of the kinetics of circular steps[18,19] were limited to unstrained crystals and, in addition, used the interaction energy of straight steps (6) instead of circular steps. In the absence of strain, the velocity dr_1/dt of the top step is directed to the center of the cone. The top step shrinks and annihilates, then the next step follows, and the island vanishes.[18,19] In contrast, the negative line energy of a step under compressive strain, which is present in the first term of Eq. (46), causes the top step to expand and hence the island to grow.

The smallest nucleus in the present model is two atomic layers high, since the model is based on step-step interactions and does not handle a single step. We simulated the island growth by numerically solving Eq. (45) for two-layer-high nuclei of different step radii r_1, r_2 and found that the nucleus has to be large enough to give rise to three-dimensional growth. For $h/l_0 = 0.2$ we found that, if the bottom step radius r_2 is smaller than $1.3l_0$, the radius of the top step r_1 decreases in time, so that the growth of such a small nucleus consists in increasing of the radius of the bottom step while the top one shrinks and vanishes. In other words, the three-dimensional growth does not begin despite the energy of the nucleus is negative: the energy is reduced further by transforming the nucleus into a two-dimensional single-step height island. With the value $l_0 \approx 3.3a$ obtained in Sec. III for single-layer S_B steps in the Ge/Si(001) system, the smallest nucleus contains $\pi(3.3\times 1.3)^2 \approx 58$ atoms. This result is in a qualitative agreement with recent experimental studies[49,50] which show that the growth of strained three-dimensional islands requires a nucleus consisting of some hundreds of atoms.

As the three-dimensional island grows, its top terrace increases in size, and a new monolayer-height island may nucleate on it. The theories of nucleation of two-dimensional islands (see Ref. 51 and references therein) cannot be applied to the present problem since they consider adatoms delivered by a deposition flux, which is neglected in our model, and do not take into account the equilibrium adatom concentration at the steps, which is a driving force for step motion in our model. On the other hand, when we attempt to create a small (compared to the characteristic distance between steps l_0) two-dimensional island on the top terrace, we find that it tends to shrink if the top terrace is not large enough (typically a few times larger than l_0). Therefore, successful nucleation is limited by the size of the top terrace and, if the nucleation proceeds faster than the step motion, the proposed model of island growth is insensitive to the nucleation mechanism and the nucleus size: the step surrounding the two-dimensional nucleus on the top terrace is able to expand only if the top terrace is sufficiently large.

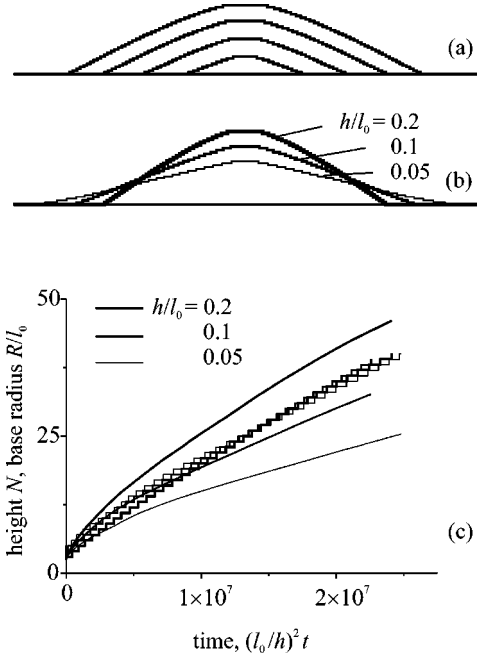

FIG. 7. Island shapes (a),(b) and time dependence of the island height and base width (c) in the model of growth kinetics: (a) shapes of islands 10, 20, 30, and 40 atomic layers high, $h/l_0 = 0.2$, (b) island shapes with of the same volume $v = 2.75\times10^6 h^3$ for different ratios h/l_0, and (c) time evolution of island dimensions, with the time t scaled as $(l_0/h)^2 t$.

Thus, the growth of a three-dimensional island is modeled as follows. The growth kinetics is obtained by numerical solution of Eqs. (45), (46), and (26). We start with a nucleus consisting of two steps which is able to grow, as described above. As soon as the radius of the top terrace exceeds $0.5l_0$, we attempt to create an additional two-dimensional island bounded by a step of radius $0.1l_0$. If it tends to shrink (i.e., $dr_1/dt < 0$), it is discarded; if it tends to expand, it is retained. We have checked that the island growth kinetics is insensitive to the nucleation parameters listed above.

Figure 7 presents the results of the kinetics calculations. Figure 7(a) shows snapshots of the growing island at heights of 10, 20, 30, and 40 atomic layers. The snapshots are taken just before the next step is successfully (i.e., with subsequent expansion) created. The radius of the top terrace varies from $3.1l_0$ for the 10-layer island to $5.8l_0$ for the 40-layer island, which makes the model insensitive to the nucleation parameters, as described above. The island shapes obtained in the kinetic model can be compared with those obtained from

energy minimization, Fig. 6(a). In both cases, the islands possess a flat top and steep sides, which is a result of the strain relaxation at the top and strain concentration at the base. The surface of the energy-minimizing island is about 2 times steeper compared to that of the island obtained from the kinetic model, as can be seen from the inset in Fig. 5 where the islands are shown with a common scale.

The distance between steps at the island base obtained in the kinetic model does not change when the island volume is increased and remains approximately equal to l_0, so that the slope is $\theta \approx h/l_0$. Using the values for the Ge/Si(001) system obtained in Sec. III, we find $\theta \approx 0.1$ for S_B steps ($h = a/\sqrt{8}, l_0 = 3.3a$) and $\theta \approx 0.3$ for D_B steps ($h = 2a/\sqrt{8}, l_0 = 2.2a$), to be compared with the surface slope of the experimentally observed Ge/Si(001) islands of $\theta \approx 0.2$. Figure 7(b) compares the shapes of the islands grown at different misfits ε_0 (the ratio h/l_0 varies proportional to ε_0). The larger misfit gives rise to a steeper island base and a larger top terrace, similar to the energy-minimized islands in Fig. 6(b).

Figure 7(c) presents the temporal evolution of the island height and base width. Calculations performed for different misfits are combined in a common plot by scaling the time by $(l_0/h)^2$. The island height is represented by the number of steps N and displayed by zigzag lines simply because N is an integer. The radii R of the island base are shown by the smooth lines. The calculations presented in the figure are performed for diffusion-limited kinetics, $l_K = 0$. We found that the kinetic coefficient K has very little influence on the growth kinetics and the results for attachment-limited kinetics ($l_K \to \infty$) only slightly differ from these for diffusion-limited kinetics.

The observations of fairly narrow island size distributions[52–56] gave rise to a theoretical controversy on the presence[6,7,54] or absence[3–5] of an energy minimum at an intermediate island size. Recent experimental observations of single-island kinetics[56–58] show that the island growth is continuous, but it essentially slows down as the island sizes increase. Our model gives a continuous decrease of the island energy during its growth and continuous increase of its sizes. We do not find, however, a slowing of the growth. Thus, the present model is not sufficient in this respect and further development of the growth kinetics model is required.

IX. CONCLUSIONS

We have shown that the results of atomistic calculations,[16] giving a negative line energy of surface steps under compressive strain, can be explained in terms of linear elasticity as an interaction of the strain produced by the step with the uniform bulk strain. The line energy of a step on a strained surface can be expressed through the dipole strength of the step in the absence of strain. We used the results of atomistic calculations of step energies on the Si(001) surface without strain[26] to obtain the dipole strengths and then were able to determine the line energies of steps under strain. These energies are in good agreement with the results of atomistic calculations[16] for different types of steps on Si(001), which confirms our approach.

We have shown that the energy of a vicinal surface can be lower, under the action of strain, than the energy of the singular surface. We have estimated the miscut angle which corresponds to a minimum of the surface energy and found that this angle amounts to a few degrees for steps on Si(001).

The energy of a singular facet can be lowered under strain by generating steps with the negative line energy. Such a mechanism of instability of strained surfaces is qualitatively different from that above the roughening transition.[33–35] First, the step energy linearly depends on the strain. It is negative for compressive strain and the instability develops only in this case. Second, there is no critical wavelength — periodic undulations consisting of steps decrease the energy at any undulation period. The period corresponding to the energy minimum increases with the amplitude of the undulation, with the slope being approximately constant proportional to the strain.

The surfaces of Stranski-Krastanov islands in systems with small and moderate misfits make sufficiently small angles with the substrate to treat them as vicinal surfaces. We presume that even the prominent (105) facets of Ge islands on Si(001) making an angle of 11° to the substrate can be qualitatively treated as vicinal. For the purpose of analytical calculations, we have considered axially symmetric islands consisting of coaxial circular steps. This approximation is as accurate as the approximation of a pyramidal island where the effects of edges are neglected.[3] The treatment of the monopole-monopole interaction between steps in our model is equivalent to the small-slope approximation in the evaluation of the elastic energy.[3–5,12,13]

The stress relaxation at the island top and the stress concentration at its base are evaluated as the sum of stress fields of the steps. The strain and stress are expressed in quadratures and can be calculated more easily than it can be done with the aid of the finite-element method. The stress relaxation has a twofold effect in our model: the line energies of steps become smaller at the island top since they are proportional to the strain and the monopole strengths of the steps also become smaller at the island top since they are proportional to the stress. The distances between steps are not equal: faceting is not inherent to our model. It can be considered as an effect of the surface reconstruction which makes the equal distances between steps favorable. We model faceting by assuming that the surface has a constant slope or consists of two segments with constant slope. In the latter case we find that the top part of the island has a smaller slope, as a result of the stress relaxation. The flatter island top and steeper base develop with increasing misfit, which is in agreement with the shapes of experimentally observed islands. We expect that atomistic calculations of energies of vicinal facets, which can be performed similarly to the calculations of energies of low-index facets under strain,[11] will give insight into island shapes in systems with smaller misfits.

We propose a model of island growth based on the Burton-Cabrera-Frank step kinetics model. The growth of a three-dimensional island requires material transport to the island top where it can be used to form a new atomic layer. This is provided by attachment of adatoms to steps from the

down terrace and detachment to the up terrace, to ensure an equilibrium adatom concentration at the step. The adatoms on the top terrace can nucleate a new two-dimensional island bounded by the circular step. We find that a newly created step is able to expand only if the terrace underneath is large enough; otherwise, it shrinks and disappears. This makes the model insensitive to the details of the nucleation process and the size of the nucleus. The slope of the island obtained in the kinetic model is about 2 times smaller than the slope of the island obtained by energy minimization.

Our calculations show that both surface undulations and three-dimensional islands reduce the energy, primarily because of the negative line energy of steps under strain. The kinetic model shows that very small nuclei bounded by two circular steps do not lead to three-dimensional growth. Rather, the top step shrinks and disappears while the bottom one grows as a two-dimensional island. A minimum nucleus allowing the growth of a three-dimensional island is estimated to contain about 60 atoms. These results are in a qualitative agreement with experiments[43,44,49,50,59,60] revealing nucleationless formation of ripples in the case of low misfit and nucleation of islands at large misfit.

ACKNOWLEDGMENT

This work was supported by the Deutsche Forschungsgemeinschaft (DFG) under Program No. SFB 296.

[1] D. J. Eaglesham and M. Cerullo, Phys. Rev. Lett. **64**, 1943 (1990).
[2] Y.-W. Mo, D. E. Savage, B. S. Swartzentruber, and M. G. Lagally, Phys. Rev. Lett. **65**, 1020 (1990).
[3] J. Tersoff and R. M. Tromp, Phys. Rev. Lett. **70**, 2782 (1993); J. Tersoff and F. K. LeGoues, *ibid.* **72**, 3570 (1994).
[4] I. Daruka, J. Tersoff, and A.-L. Barabási, Phys. Rev. Lett. **82**, 2753 (1999).
[5] B. J. Spencer and J. Tersoff, Phys. Rev. Lett. **79**, 4858 (1997).
[6] V. A. Shchukin, N. N. Ledentsov, P. S. Kop'ev, and D. Bimberg, Phys. Rev. Lett. **75**, 2968 (1995).
[7] I. Daruka and A.-L. Barabási, Phys. Rev. Lett. **79**, 3708 (1997).
[8] S. Christiansen, M. Albrecht, H. P. Strunk, and H. J. Maier, Appl. Phys. Lett. **64**, 3617 (1994); S. Christiansen, M. Albrecht, H. P. Strunk, P. O. Hansson, and E. Bauser, *ibid.* **66**, 574 (1995); S. Christiansen, M. Albrecht, and H. P. Strunk, Comput. Mater. Sci. **7**, 213 (1996).
[9] H. T. Johnson and L. B. Freund, J. Appl. Phys. **81**, 6081 (1997).
[10] D. E. Jesson, G. Chen, K. M. Chen, and S. J. Pennycook, Phys. Rev. Lett. **80**, 5156 (1998).
[11] E. Pehlke, N. Moll, A. Kley, and M. Scheffler, Appl. Phys. A: Mater. Sci. Process. **65**, 525 (1997); L. G. Wang, P. Kratzer, M. Scheffler, and N. Moll, Phys. Rev. Lett. **82**, 4042 (1999); Q. K. K. Liu, N. Moll, M. Scheffler, and E. Pehlke, Phys. Rev. B **60**, 17 008 (1999); L. G. Wang, P. Kratzer, N. Moll, and M. Scheffler, *ibid.* **62**, 1897 (2000).
[12] H. Gao, J. Mech. Phys. Solids **39**, 443 (1991).
[13] L. B. Freund, Acta Mech. Sin. **10**, 16 (1994); Int. J. Solids Struct. **32**, 911 (1995).
[14] D. Lacombe, A. Ponchet, S. Fréchengues, V. Drouot, N. Bertru, B. Lambert, and A. L. Corre, Appl. Phys. Lett. **74**, 1680 (1999).
[15] P. O. Hansson, M. Albrecht, W. Dorsch, H. P. Strunk, and E. Bauser, Phys. Rev. Lett. **73**, 444 (1994); W. Dorsch, S. Christiansen, M. Albrecht, P. O. Hansson, E. Bauser, and H. P. Strunk, Surf. Sci. **331-333**, 896 (1995).
[16] Y. H. Xie, G. H. Gilmer, C. Roland, P. J. Silverman, S. K. Buratto, J. Y. Cheng, E. A. Fitzgerald, A. R. Kortan, S. Schuppler, M. A. Marcus, and P. H. Citrin, Phys. Rev. Lett. **73**, 3006 (1994).
[17] W. Barvosa-Carter, M. J. Aziz, L. J. Gray, and T. Kaplan, Phys. Rev. Lett. **81**, 1445 (1998).
[18] N. Israeli and D. Kandel, Phys. Rev. Lett. **80**, 3300 (1998); Phys. Rev. B **60**, 5946 (1999).
[19] M. Uwaha and K. Watanabe, J. Phys. Soc. Jpn. **69**, 497 (2000).
[20] V. M. Kaganer and K. H. Ploog, Solid State Commun. **117**, 337 (2001).
[21] W. K. Burton, N. Cabrera, and F. C. Frank, Philos. Trans. R. Soc. London, Ser. A **243**, 299 (1951).
[22] M. Ozdemir and A. Zangwill, Phys. Rev. B **42**, 5013 (1990).
[23] M. Sato and M. Uwaha, Phys. Rev. B **51**, 11 172 (1995).
[24] L. D. Landau, in *Collected papers*, edited by D. ter Haar (Pergamon Press, Oxford, 1965), p. 540.
[25] W. W. Mullins, in *Metal Surfaces: Structure, Energetics and Kinetics*, edited by W. D. Robertson and N. A. Gjostein (American Society for Metals, Metals Park, OH, 1963), p. 17.
[26] T. W. Poon, S. Yip, P. S. Ho, and F. F. Abraham, Phys. Rev. Lett. **65**, 2161 (1990); Phys. Rev. B **45**, 3521 (1992).
[27] C. Teodosiu, *Elastic Models of Crystal Defects* (Springer, Berlin, 1982).
[28] V. I. Marchenko and A. Y. Parshin, Zh. Éksp. Teor. Fiz. **79**, 257 (1980) [Sov. Phys. JETP **52**, 129 (1980)].
[29] A. F. Andreev and Y. A. Kosevich, Zh. Éksp. Teor. Fiz. **81**, 1435 (1981) [Sov. Phys. JETP **54**, 761 (1981)].
[30] J. Stewart, O. Pohland, and J. M. Gibson, Phys. Rev. B **49**, 13 848 (1994).
[31] L. E. Shilkrot and D. J. Srolovitz, Phys. Rev. B **53**, 11 120 (1996).
[32] D. J. Chadi, Phys. Rev. Lett. **59**, 1691 (1987).
[33] R. J. Asaro and W. A. Tiller, Metall. Trans. **3**, 1789 (1972).
[34] M. A. Gringeld, Dokl. Akad. Nauk SSSR **290**, 1358 (1986) [Sov. Phys. Dokl. **31**, 831 (1986)].
[35] D. J. Srolovitz, Acta Metall. **37**, 621 (1989).
[36] B. J. Spencer, P. W. Voorhees, and S. H. Davis, Phys. Rev. Lett. **67**, 3696 (1991).
[37] B. J. Spencer, P. W. Voorhees, and S. H. Davis, J. Appl. Phys. **73**, 4955 (1993).
[38] M. Grinfeld, Phys. Rev. B **49**, 8310 (1994).
[39] A. Rettori and J. Villain, J. Phys. (Paris) **49**, 257 (1988).
[40] F. Lançon and J. Villain, Phys. Rev. Lett. **64**, 293 (1990).
[41] J. Tersoff, Y. H. Phang, Z. Zhang, and M. G. Lagally, Phys. Rev. Lett. **75**, 2730 (1995); J. Tersoff, *ibid.* **74**, 4962 (1995); F. Liu, T. Tersoff, and M. G. Lagally, *ibid.* **80**, 1268 (1998); J. Tersoff, *ibid.* **80**, 2018 (1998).

[42] L. D. Landau and E. M. Lifshitz, *Theory of Elasticity* (Pergamon Press, Oxford, 1970).
[43] P. Sutter and M. G. Lagally, Phys. Rev. Lett. **84**, 4637 (2000).
[44] R. M. Tromp, F. M. Ross, and M. C. Reuter, Phys. Rev. Lett. **84**, 4641 (2000).
[45] Y. Chen and J. Washburn, Phys. Rev. Lett. **77**, 4046 (1996).
[46] L. J. Gray, M. F. Chisholm, and T. Kaplan, Appl. Phys. Lett. **66**, 1924 (1995).
[47] W. Yu and A. Madhukar, Phys. Rev. Lett. **79**, 905 (1997).
[48] K. M. Chen, D. E. Jesson, S. J. Pennycook, T. Thundat, and R. J. Warmack, Phys. Rev. B **56**, 1700 (1997).
[49] D. E. Jesson, M. Kästner, and B. Voigtländer, Phys. Rev. Lett. **84**, 330 (2000).
[50] a. Vailionis, B. Cho, G. Glass, P. Desjardins, D. G. Cahill, and J. E. Greene, Phys. Rev. Lett. **85**, 3672 (2000).
[51] J. Krug, P. Politi, and T. Michely, Phys. Rev. B **61**, 14 037 (2000).
[52] D. Leonard, K. Pond, and P. M. Petroff, Phys. Rev. B **50**, 11 687 (1994).
[53] J. M. Moison F. Houzay, F. Barthe, L. Leprince, E. André, and O. Vatel, Appl. Phys. Lett. **64**, 196 (1994).
[54] G. Medeiros-Ribeiro, A. M. Bratkovski, T. I. Kamins, D. A. A. Ohlberg, and R. S. Williams, Science **279**, 353 (1998).
[55] S. A. Chaparro, Y. Zhang, J. Drucker, D. Chandrasekhar, and D. J. Smith, J. Appl. Phys. **87**, 2245 (2000).
[56] I. Goldfarb, P. T. Hayden, J. H. G. Owen, and G. A. D. Briggs, Phys. Rev. B **56**, 10 459 (1997).
[57] M. Kästner and B. Voigtländer, Phys. Rev. Lett. **82**, 2745 (1999).
[58] F. M. Ross, R. M. Tromp, and M. C. Reuter, Science **286**, 1931 (1999).
[59] S. H. Christiansen, H. P. Strunk, H. Wawra, M. Becker, and M. Albrecht, Solid State Phenom. **69-70**, 93 (1999).
[60] S. H. Christiansen, M. Albrecht, M. Becker, H. P. Strunk, and H. Wawra, in *Epitaxial Growth*, edited by T. P. Pearsall, A. L. Barabasi, F. Lin, and G. N. Maracas, Mater. Res. Soc. Symp. Proc. No. **570** (Materials Research Society, Pittsburgh, 1999), p. 199.